New Energy Consumption Model for Rotary-Wing UAV Propulsion

Hua Yan, *Graduate Student Member, IEEE*, Yunfei Chen, *Senior Member, IEEE*, and Shuang-Hua Yang, *Senior Member, IEEE*

***Abstract*— Accurate and convenient energy consumption models (ECMs) for rotary-wing unmanned aerial vehicles (UAVs) are important for UAV communication designs. Existing models are complex and inconvenient to use. In this letter, a simple and easy-to-use model with closed-form expression as a function of the initial velocity, acceleration and time duration is derived. Using this model, the UAV flight control parameters, such as polling force and tilt angle, are analyzed in analytical form. Numerical results show the validity and reliability of the proposed model.**

***Index Terms*—Energy consumption model (ECM), unmanned aerial vehicle (UAV), UAV communications.**

I. Introduction

PROPULSION energy consumption of unmanned aerial vehicles (UAVs) is very important in the design of UAV-enabled communications systems [1]–[3]. The challenge is to accurately estimate the amount of energy consumed by different UAV missions.

There have been quite a few works on the modeling of propulsion energy [4], [5]. For example, the authors in [6] and [7] studied the energy consumption of electric-powered UAVs, and this method has been proved effective and feasible. In [8], a theoretical model for multi-rotor small unmanned aircraft power consumption based on helicopter theory was derived assuming a steady-state without acceleration. Similarly, in [9], the authors derived a closed-form propulsion power consumption model for rotary-wing UAVs in a one-dimensional (1-D) level flight at a constant speed without acceleration/deceleration. Considering the practical situation, the authors in [10] extended the result in [9] by deriving an analytical model for rotary-wing UAVs in straight-and-level flight with acceleration and deceleration. However, this model is very complex, as no closed-form expression and only an integral expression was provided in [10, eq. (A.8)]. Also, the model in [9] was further extended in [11] to an arbitrary two-dimensional (2-D) level flight, and the energy consumption was derived as a function of the flying speed, direction and acceleration using centrifugal acceleration [12]. This model is also very complicated without closed-form.

All these works have provided very valuable insights on modeling the propulsion energy consumption of rotary-wing UAVs. However, these models are either too complex, or do not consider acceleration/deceleration—a very important UAV manoeuvrer in UAV-enabled communications [1]–[3], [9]. Thus, it is of great interest to derive a new energy consumption model (ECM) that is both simple and takes the acceleration/deceleration into account. Such an ECM can be used to calculate the energy consumed in different UAV missions, or as a target for UAV trajectory optimization.

Motivated by the above observation, this letter aims to derive a new ECM that overcomes the shortcomings of the aforementioned works. To do this, we decompose the power consumption of the UAV with acceleration/deceleration into vertical and horizontal directions using force analysis, based on which a new ECM is derived. Numerical results show the validity and reliability of the new ECM and that acceleration and speed have a great impact on the total energy consumption of the UAV. The novelty of the work is summarized as follows: compared with [9], this work considers both acceleration and deceleration, while [9] did not consider acceleration/deceleration. Compared with [10] and [11], our model is much simpler and easier to use with closed-form, while the model in [10] or [11] is complex and does not have closed-form expression.

II. Existing Energy Consumption Models

From [9], for forward level flight of a rotary-wing UAV at a constant speed of *V*, the propulsion power consumption can be modeled as

$$P(V,\widetilde{\kappa}) = P_0\left(1+\frac{3V^2}{U_{tip}^2}\right) + P_1\widetilde{\kappa}\left(\sqrt{\widetilde{\kappa}^2+\frac{V^4}{4v_0^2}}-\frac{V^2}{2v_0^2}\right)^{\frac{1}{2}} + \frac{d_0\rho s A V^3}{2}, \tag{1}$$

where $P_0\left(1+\frac{3V^2}{U_{tip}^2}\right)$ and $P_1\widetilde{\kappa}\left(\sqrt{\widetilde{\kappa}^2+\frac{V^4}{4v_0^2}}-\frac{V^2}{2v_0^2}\right)^{1/2}$ are functions of speed related to the physical properties of the UAV and the flight environment, including the UAV weight *W*, rotor solidity *s*, rotor disc area *A*, air density ρ, the tip speed of the rotor blade U_{tip} and the mean rotor induced velocity v_0, etc., as the *blade profile power* and *induced power* in hovering status, as detailed in [9], $\widetilde{\kappa} \triangleq \frac{T}{W} \approx 1$ is the thrust-to-weight ratio (TWR) [13, eq. (4.3)], d_0 denotes the fuselage drag ratio and $d_0\rho s A V^3/2$ denotes the *parasite power* (also known as power to overcome fuselage drag [13, eq. (4.5)] related to speed). Therefore, the energy consumption can be modeled as a function of *V*, which is neither convex nor concave, similar

Manuscript received May 13, 2021; accepted June 15, 2021. Date of publication June 21, 2021; date of current version September 9, 2021. This work was supported in part by the National Key Research and Development Program of China under Grant 2019YFC0810705; in part by the National Natural Science Foundation of China under Grant 61873119 and Grant 92067109; and in part by the Science and Technology Innovation Commission of Shenzhen under Grant KQJSCX20180322151418232. The associate editor coordinating the review of this article and approving it for publication was A. A. Nasir. *(Corresponding author: Shuang-Hua Yang.)*

Hua Yan and Yunfei Chen are with the School of Engineering, University of Warwick, Coventry CV4 7AL, U.K. (e-mail: hua.yan@warwick.ac.uk; yunfei.chen@warwick.ac.uk).

Shuang-Hua Yang is with the Department of Computer Science and Engineering, Southern University of Science and Technology, Shenzhen 518055, China, and also with PCL Research Center of Networks and Communications, Peng Cheng Laboratory, Shenzhen 518055, China (e-mail: yangsh@sustech.edu.cn).

Digital Object Identifier 10.1109/LWC.2021.3090772

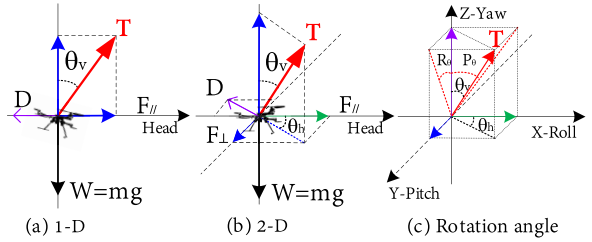

Fig. 1. Force analysis of the UAV.

to [9]. Using (1), one has

$$E_v = P(V, 1)\tau, \tag{2}$$

where τ is the time duration and $\widetilde{\kappa} = 1$.

From [10], for forward level flight, with a given trajectory $q(t)$, the propulsion energy is calculated as

$$\begin{aligned} E(q(t), T_0) = &\int_0^{T_0} [P_0\big(1 + c_1 v^2(t)\big) + c_5 v^3(t) \\ &+ P_1\sqrt{1 + (c_2 v^2(t) + c_3 a(t)v(t))^2} \\ &\times \sqrt{\sqrt{1 + (c_2 v^2(t) + c_3 a(t)v(t))^2 + c_4^2 v^4(t)} - c_4 v^2(t)}]\, dt, \end{aligned} \tag{3}$$

where T_0 is the time duration, $c_j, j = 1, \ldots, 5$, are the parameters detailed in [10], $v(t) = \frac{dq(t)}{dt}$ and $a(t) = \frac{d^2 q(t)}{dt^2}$ are the velocity and acceleration, respectively.

Also, from [11], for an arbitrary 2-D level flight with given trajectory $\mathbf{q}(t)$, the propulsion energy is presented as

$$\begin{aligned} &E(\mathbf{q}(t)) \\ &= \int_0^{T_0} c_3\sqrt{1 + \frac{a_\perp^2(t)}{g^2}}\left(\sqrt{1 + \frac{a_\perp^2(t)}{g^2} + \frac{\|\mathbf{v}(t)\|^4}{c_4^2}} - \frac{\|\mathbf{v}(t)\|^2}{c_4}\right)^{\frac{1}{2}} dt \\ &\quad + \int_0^{T_0} c_1(1 + c_2\|\mathbf{v}(t)\|^2)\, dt + \int_0^{T_0} c_5\|\mathbf{v}(t)\|^3\, dt + \Delta_K, \end{aligned} \tag{4}$$

where T_0 is the time duration, $c_k, k = 1, \ldots, 5$ are the parameters detailed in [11], $\Delta_K = \frac{1}{2}m(\|\mathbf{v}(T_0)\|^2 - \|\mathbf{v}(0)\|^2)$ is the change in kinetic energy. Both (3) and (4) are very complex to use and do not have closed-form expression.

III. New Energy Consumption Model

In this section, we will study the power consumption of UAV with acceleration/deceleration from the initial velocity $\mathbf{V}_i$ (final velocity $\mathbf{V}_f$) to $\mathbf{V}_f(\mathbf{V}_i)$. Using the same parameters as those in [9] to derive the new model. Since the 1-D scenario is a special case of the 2-D scenario, we will focus on 2-D scenarios to derive a generic model.

As indicated in (1), for forward level flight, the UAV keeps balance in the vertical direction at the cost of *blade profile power* and *induced power*. On the other hand, in the horizontal direction, the UAV incurs the fuselage drag, i.e., *parasite power*. Based on this analysis, the required power consumption for a rotary-wing UAV can be studied by analyzing the vertical and horizontal power consumption. In the vertical direction, the UAV keeps balance at the cost of $P_0(1 + \frac{3V^2}{U_{tip}^2}) + P_1\widetilde{\kappa}(\sqrt{\widetilde{\kappa}^2 + \frac{V^4}{4v_0^2}} - \frac{V^2}{2v_0^2})^{1/2}$. During acceleration/deceleration, $\widetilde{\kappa} = \sqrt{1 + \frac{(\rho S_{FP} V^2 + 2ma)^2}{4W^2}}$ [10, eq. (A.5)], and $S_{FP} \triangleq d_0 sA$ [9] is the fuselage equivalent flat plate area. Using the parameters from [9, Table I] with a maximum speed of $V_{max} = 30\ m/s$ [9], it is found that $\widetilde{\kappa}$ approximately equals to 1 for different accelerations and UAV weights. As a result, the power consumption for acceleration/deceleration in vertical direction can be expressed as

$$\begin{aligned} P_{vertical}(t) = &P_0\left(1 + \frac{3\|\mathbf{V}_i + \mathbf{a}t\|^2}{U_{tip}^2}\right) \\ &+ P_1\left(\sqrt{1 + \frac{\|\mathbf{V}_i + \mathbf{a}t\|^4}{4v_0^4}} - \frac{\|\mathbf{V}_i + \mathbf{a}t\|^2}{2v_0^2}\right)^{\frac{1}{2}}, \end{aligned} \tag{5}$$

where $\mathbf{V}_i$ is the initial velocity and $\mathbf{a}$ is the acceleration or deceleration. Thus, $P_{vertical}(t)$ varies with the UAV speed, and it is not related to the orientation. In the horizontal direction, the power consumption at a speed of $\mathbf{v}(t)$ is [12]

$$P_{horizontal}(t) = \|\mathbf{F}\|\|\mathbf{v}(t)\|, \tag{6}$$

where $\mathbf{F}$ is the pulling force, $\mathbf{v}(t) = \|\mathbf{V}_i + \mathbf{a}t\|$ is the instantaneous velocity at time t. When flying at a constant speed of V, $\|\mathbf{F}\| = \frac{1}{2}d_0\rho sAV^2$ equals to the fuselage drag $D = \frac{1}{2}\rho S_{FP} V^2$ [13]. According to the above analysis, the power consumption for rotary-wing UAVs can be finally modeled as

$$P_{total}(t) = P_{vertical}(t) + P_{horizontal}(t). \tag{7}$$

Particularly, when $\|\mathbf{a}\| = 0$, (7) is the same as $P(V, 1)$ in (1) and [9, eq. (12)]. Thus, (7) is general.

A. Acceleration/Deceleration

From [11] and [12], the UAV acceleration can be decomposed in the parallel and perpendicular directions of its head. Considering an arbitrary 2-D level flight with acceleration $\mathbf{a}$ shown in Fig. 1(b), one has

$$\begin{aligned} T\sin\theta_v\cos\theta_h - D_{\shortparallel} &= ma_{\shortparallel}, \\ T\sin\theta_v\sin\theta_h - D_\perp &= ma_\perp, \\ T\cos\theta_v - W &= 0, \end{aligned} \tag{8}$$

where m is the total mass of the UAV, θ_h is the initial angle between $\mathbf{a}$ and $\mathbf{V}_i$ and it can be derived by rotation of the UAV, i.e., rotation of angle P_θ along pitch and angle R_θ along roll. One has the relationship as

$$\theta_h = \arctan\left(\frac{\tan R_\theta}{\tan P_\theta}\right), \tag{9}$$

$D_{\shortparallel} = \frac{1}{2}\rho S_{FP} v_{\shortparallel}^2(t)$ and $D_\perp = \frac{1}{2}\rho S_{FP} v_\perp^2(t)$ are the fuselage drags in the parallel and perpendicular directions, $a_{\shortparallel} = \|\mathbf{a}\|\cos\theta_h$ and $a_\perp = \|\mathbf{a}\|\sin\theta_h$ are acceleration components that are parallel and perpendicular to the head direction [11], [12], respectively. Using (6) and (8), the power in parallel and perpendicular directions for arbitrary 2-D level acceleration is

$$\begin{aligned} P_{\shortparallel}(t) &= \left(\frac{1}{2}\rho S_{FP} v_{\shortparallel}^2(t) + ma_{\shortparallel}\right)v_{\shortparallel}(t), \\ P_\perp(t) &= \left(\frac{1}{2}\rho S_{FP} v_\perp^2(t) + ma_\perp\right)v_\perp(t), \end{aligned} \tag{10}$$

where $v_{\shortparallel}(t) = v_{i\shortparallel} + a_{\shortparallel}t$ and $v_\perp(t) = v_{i\perp} + a_\perp t$ are speed components that are parallel and perpendicular to the head,

respectively, $v_{i\shortparallel} = \|\mathbf{V}_i\|\cos\theta_h$ and $v_{i\perp} = \|\mathbf{V}_i\|\sin\theta_h$ are two components of initial velocity $\mathbf{v}_0$ in the corresponding direction. Using (7) and (10), the total power consumption is

$$P_{total-2D}(t) = P_{vertical}(t) + P_{\shortparallel}(t) + P_{\perp}(t). \quad (11)$$

Since the deceleration process is similar to the acceleration process, it will not be repeated here. Together, the total energy for accelerating/decelerating with initial $\mathbf{V}_i$, acceleration/deceleration $\mathbf{a}$ during a time period of τ, using (11), is

$$\begin{aligned} E_{2D}(\mathbf{V}_i,\mathbf{a},\tau) &= \int_0^{\tau} P_{total-2D}(t)\ dt \\ &= P_0\tau + \frac{3P_0}{U_{tip}^2}\left(\|\mathbf{V}_i\|^2\tau + \|\mathbf{V}_i\|\|\mathbf{a}\|\cos\theta_h\tau^2 + \frac{\|\mathbf{a}\|^2\tau^3}{3}\right) \\ &\pm\frac{P_1 v_0}{2\|\mathbf{a}\|}\left(\ln\frac{\left(2v_0^2+\xi I_u+2v_0\sqrt{\Re_u}\right)I_l}{I_u\left(2v_0^2+\xi I_l+2v_0\sqrt{\Re_l}\right)}\right) \\ &\pm\frac{P_1}{2\|\mathbf{a}\|}\left(\sqrt{\Re_u}-\sqrt{\Re_l}+\frac{\xi}{2v_0}(\arcsin\Im_u-\arcsin\Im_l)\right) \\ &+\frac{1}{2}\rho S_{FP}\Phi(\tau)\pm ma_{\shortparallel}v_{i\shortparallel}\tau+\frac{1}{2}ma_{\shortparallel}^2\tau^2 \\ &+\frac{1}{2}\rho S_{FP}\Psi(\tau)\pm ma_{\perp}v_{i\perp}\tau+\frac{1}{2}ma_{\perp}^2\tau^2, \end{aligned} \quad (12)$$

where $I_u = \sqrt{1+\frac{(\|\mathbf{V}_i+\mathbf{a}\tau\|)^4}{4v_0^4}} - \frac{(\|\mathbf{V}_i+\mathbf{a}\tau\|)^2}{2v_0^2}$, $I_l = \sqrt{1+\frac{\|\mathbf{V}_i\|^4}{4v_0^4}} - \frac{\|\mathbf{V}_i\|^2}{2v_0^2}$, $\xi = \|\mathbf{V}_i\|^2\cos^2\theta_h - \|\mathbf{V}_i\|^2$, $\Re_u = -v_0^2I_u^2+\xi I_u+v_0^2$, $\Re_l = -v_0^2I_l^2+\xi I_l+v_0^2$, $\Im_u = \frac{-2v_0^2I_u+\xi}{\sqrt{\xi^2+4v_0^4}}$, $\Im_l = \frac{-2v_0^2I_l+\xi}{\sqrt{\xi^2+4v_0^4}}$, $\Phi(\tau) = v_{i\shortparallel}^3\tau \pm \frac{3}{2}v_{i\shortparallel}^2a_{\shortparallel}\tau^2 + v_{i\shortparallel}a_{\shortparallel}^2\tau^3 \pm \frac{1}{4}a_{\shortparallel}^3\tau^4$, $\Psi(\tau) = v_{i\perp}^3\tau \pm \frac{3}{2}v_{i\perp}^2a_{\perp}\tau^2 + v_{i\perp}a_{\perp}^2\tau^3 \pm \frac{1}{4}a_{\perp}^3\tau^4$, $\tau = \frac{\|\mathbf{v}_f-\mathbf{v}_i\|}{\|\mathbf{a}\|}$ is the acceleration/deceleration time, and the plus and minus sign "±" corresponds to the total energy of acceleration and deceleration processes (and hereinafter) denoted by E_{2D-Acc} and E_{2D-Dec}, respectively.

As a special case of the 2-D scenario, the ECM for 1-D level flight when $\theta_h = 0$ or π can be derived as

$$\begin{aligned} E_{1D}(\mathbf{V}_i,\mathbf{a},\tau) &= P_0\tau + \frac{3P_0}{U_{tip}^2}\left(\|\mathbf{V}_i\|^2\tau \pm \|\mathbf{V}_i\|\|\mathbf{a}\|\tau^2 + \frac{\|\mathbf{a}\|^2\tau^3}{3}\right) \\ &\pm\frac{P_1 v_0}{2\|\mathbf{a}\|}\left(\ln\frac{\left(1+\sqrt{1-I_u^2}\right)I_l}{I_u\left(1+\sqrt{1-I_l^2}\right)} + \sqrt{1-I_u^2} - \sqrt{1-I_l^2}\right) \\ &+\frac{1}{2}\rho S_{FP}\Omega(\tau)\pm ma\|\mathbf{V}_i\|\tau+\frac{1}{2}ma^2\tau^2, \end{aligned} \quad (13)$$

where $a = \|\mathbf{a}\|$, $\Omega(\tau) = \|\mathbf{V}_i\|^3\tau \pm \frac{3}{2}\|\mathbf{V}_i\|^2a\tau^2 + \|\mathbf{V}_i\|a^2\tau^3 \pm \frac{1}{4}a^3\tau^4$.

Compared with the existing models, our model has a close-form expression and has taken acceleration/deceleration at directions that are parallel and perpendicular to the UAV head into account. Therefore, it is more reasonable and practical.

B. Further Discussion

1) Analysis of Manoeuvring Parameters: During acceleration/deceleration, T, tilt angle θ_v (also known as rotation angle P_θ along pitch in Fig. 1(c)) and θ_h change with the speed, as

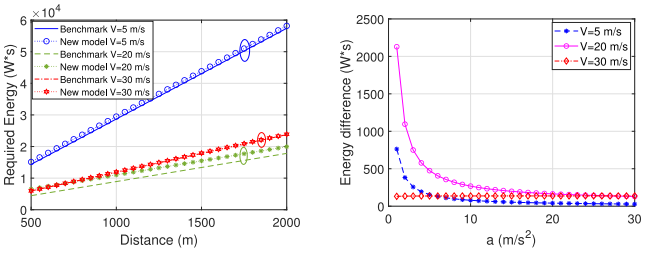

(a) Total energy consumption. (b) Energy gap caused by acceleration.

Fig. 2. New model VS [9].

D is proportional to the speed, and one has

$$T(t) = W\times\sqrt{1+\frac{\left(\rho S_{FP}(\|\mathbf{V}_i+\mathbf{a}t\|)^2+2m\|\mathbf{a}\|\right)^2}{4W^2}},$$
$$\theta_v(t) = \arctan\frac{\rho S_{FP}(\|\mathbf{V}_i+\mathbf{a}t\|)^2+2m\|\mathbf{a}\|}{2W}. \quad (14)$$

2) Special Case: Considering an *acceleration-fly(V)-deceleration* operation [1], [2] of 1-D scenarios, where the UAV accelerates from an initial velocity of 0 to V and continues to fly at the speed of V, and finally decelerates from V to 0. The total energy, using (2) and (13), can be calculated as

$$E = E_{1D}(0,\mathbf{a}_1,\tau_1) + E_v + E_{1D}(V,\mathbf{a}_2,\tau_2). \quad (15)$$

where $\tau_1 = \frac{\|\mathbf{V}\|}{\|\mathbf{a}_1\|}$ and $\tau_2 = \frac{\|\mathbf{V}\|}{\|\mathbf{a}_2\|}$. Note that, for a given distance d, E_v exists if and only if $d > \frac{\|\mathbf{v}\|^2}{2\|\mathbf{a}_1\|} + \frac{\|\mathbf{v}\|^2}{2\|\mathbf{a}_2\|}$.

IV. Numerical Results and Discussion

In this section, numerical examples are given to validate the derived energy model by comparing it with the models in [9], [10], [11]. Also, for a given distance, we compare the total energy calculated by the new model considering acceleration and deceleration with that calculated by the benchmark model [9] without considering acceleration or deceleration. For acceleration, the new model is also compared with [10] and [11]. In the examples, we set $W = 20\ N$ [9], $a = \pm 1\ m/s^2$, the number of wings and the number of blades are 4, and other parameters of UAV are the same as given in [9, Table I].

Fig. 2(a) shows the total energy consumption versus the distance for different speeds in 1-D. One sees that the total energy consumption increases with the distance, but decreases first and then increases with the speed. This is because, when the speed is low, the power consumption is relatively large [9]. As both acceleration and deceleration have been considered in the new model, one can also see that the energy calculated by the new model is larger than that from [9]. For fixed distance at 1500 m, one can see that, when the speed is small (5 m/s) or large (30 m/s), the new model and the model in [9] match better than when the speed is medium. This is due to acceleration, which prolongs the acceleration process to consume more energy.

Fig. 2(b) shows the energy gap between the new model and the model in [9]. In this figure, we fix the distance at 2000 m and vary the acceleration from 1 to 30 m/s^2. One sees that for the speed V changing from 5 m/s to 20 m/s, the gap decreases with the acceleration. This can be explained as follows. For small a, the acceleration/deceleration process increases and

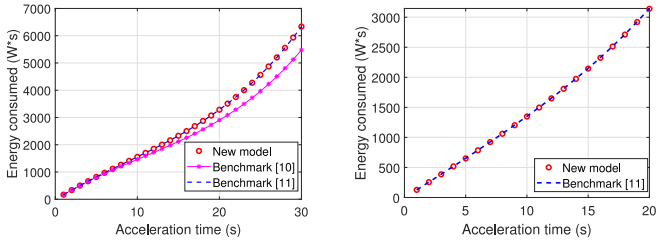

(a) 1D scenario. (b) 2D scenario.

Fig. 3. New model VS [10] and [11].

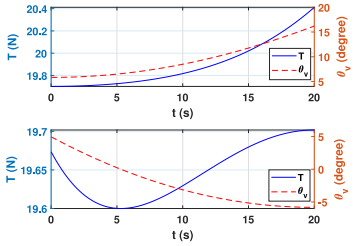

Fig. 4. T and θ_v change with t in the process of acceleration/deceleration from $v_0(v)$ to $v(v_0)$.

the power consumption is relatively large when the speed is low [9] so as to consume more energy; For large a, the time for acceleration/deceleration is short, the energy gap becomes stable. Besides, for fixed a, the energy gap increases with the speed first and then decreases as in Fig. 2(a). When the speed is set as 30 *m/s*, which is larger than the *maximum − range* (*MR*) *speed* [9], the energy gap changes little with the acceleration. This is due to the fact that, when the speed is larger than the *MR* speed, higher power consumption is needed [9] so that the difference caused by acceleration is relatively small compared with the total energy consumption. This is why the new model and the model in [9] match well when the speed is 30 *m/s*.

Fig. 3(a) compares the total energy consumption of the new model with those in [10] and [11]. In the figure, (13), [10, eq. (A.8)] and [11, eq. (4)] are used, $a = 1\ m/s^2$, and other parameters are the same as [9, Table 1]. One can see that the energy consumption increases with the acceleration time, and the energy consumption calculated by the new model is the same as that calculated by [11, eq. (4)]. However, [11, eq. (4)] is complex to use and does not have closed-form expression. In [10], even if D is considered, the pull force T could remain unchanged so as to cause the change of a, i.e., $a < 1\ m/s^2$ as time goes on. In our work, D increases with the acceleration time so that T also increases to keep a. As a result, it consumes more energy. Note that when the speed is small, D is also small. This is why the three curves overlap at the beginning.

Fig. 3(b) investigates the total energy consumption of the new model and that in [11] for a 2D case. In the figure, (12) is used and $v_{\shortparallel} = 10\ m/s$, $a_{\shortparallel} = 0\ m/s^2$, $v_{\perp} = 0\ m/s$, $a_{\perp} = 1\ m/s^2$. One sees that two curves match well, similar to Fig. 3(a). However, [11, eq. (4)] does not have closed-form expression, and acceleration/deceleration that is parallel to the UAV head direction has been largely ignored.

Fig. 4 shows the change of the pulling force T and tilt angle θ_v using (14). For acceleration, one can see that both T and θ_v increase with t. This is because the fuselage drag increases with the speed during the acceleration process, leading to a gradually increasing T to maintain a. Meanwhile, in order to balance the UAV weight in vertical direction, i.e., $T\cos\theta_v = W$ in (8), θ_v also needs to be increased accordingly. For deceleration, one sees that T decreases first and then increases, while θ_v changes from the velocity direction to the deceleration direction. This can be explained as follows. When the UAV is flying at speed of $v = 20$ *m/s*, its fuselage drag is $D = \frac{1}{2}\rho S_{FP} v^2$, this drag is large enough to make a deceleration of more than $a = 1\ m/s^2$. Thus, a certain amount of T in the same direction of the speed is still needed. However, with the decreasing speed, D gradually decreases. Hence, T also needs to decrease in the direction of the speed. This is why T decreases from time 0 to the 5^{th} second. Also, for balancing the UAV weight, θ_v decreases accordingly. From the figure, when it's nearly the 5^{th} second, T starts to increase. This is because D is not large enough to make a deceleration of $a = 1\ m/s^2$. Hence, a certain amount of T in the opposite direction of the speed is needed. As shown in the figure, the curve representing θ_v changes from positive to negative, which indicates the direction change of T. As T continues to increase, θ_v also needs to be increased, showing a downward curve from 0 to -5.

V. Conclusion

A new ECM considering both acceleration and deceleration as a function of acceleration and time duration has been derived. Numerical results have shown the validity and reliability of the new ECM. The effects of wind and variable acceleration are also important but will be considered as future work due to length limit.

References

[1] H. Yan, Y. Chen, and S.-H. Yang, "Analysis of energy transfer efficiency in UAV-enabled wireless networks," *Phys. Commun.*, vol. 37, Dec. 2019, Art. no. 100849.

[2] H. Yan, Y. Chen, and S.-H. Yang, "UAV-enabled wireless power transfer with base station charging and UAV power consumption," *IEEE Trans. Veh. Technol.*, vol. 69, no. 11, pp. 12883–12896, Nov. 2020.

[3] H. Yan, S.-H. Yang, Y. Chen, and S. A. Fahmy, "Optimum battery weight for maximizing available energy in UAV-enabled wireless communications," *IEEE Wireless Commun. Lett.*, early access, Mar. 26, 2021, doi: 10.1109/LWC.2021.3069078.

[4] J. Zhang, J. F. Campbell, D. C. Sweeney, and A. C. Hupman, "Energy consumption models for delivery drones: A comparison and assessment," *Transp. Res. D, Transp. Environ.*, vol. 90, Jan. 2021, Art. no. 102668.

[5] A. Thibbotuwawa, P. Nielsen, B. Zbigniew, and G. Bocewicz, "Energy consumption in unmanned aerial vehicles: A review of energy consumption models and their relation to the UAV routing," in *Advances in Intelligent Systems and Computing*, vol. 853. Cham, Switzerland: Springer-Verlag, 2019, pp. 173–184.

[6] C. W. Chan and T. Y. Kam, "A procedure for power consumption estimation of multi-rotor unmanned aerial vehicle," in *J. Phys. Conf. Series*, vol. 1509, no. 1, Apr. 2020, Art. no. 012015.

[7] H. V. Abeywickrama, B. A. Jayawickrama, Y. He, and E. Dutkiewicz, "Comprehensive energy consumption model for unmanned aerial vehicles, based on empirical studies of battery performance," *IEEE Access*, vol. 6, pp. 58383–58394, 2018.

[8] Z. Liu, R. Sengupta, and A. Kurzhanskiy, "A power consumption model for multi-rotor small unmanned aircraft systems," in *Proc. Int. Conf. Unmanned Aircr. Syst.*, Jul. 2017, pp. 310–315.

[9] Y. Zeng, J. Xu, and R. Zhang, "Energy minimization for wireless communication with rotary-wing UAV," *IEEE Trans. Wireless Commun.*, vol. 18, no. 4, pp. 2329–2345, Apr. 2019.

[10] Z. Yang, W. Xu, and M. Shikh-Bahaei, "Energy efficient UAV communication with energy harvesting," *IEEE Trans. Veh. Technol.*, vol. 69, no. 2, pp. 1913–1927, Feb. 2020.

[11] N. Gao *et al.*, "Energy model for UAV communications: Experimental validation and model generalization," May 2020. [Online]. Available: http://arxiv.org/abs/2005.01305

[12] Y. Zeng and R. Zhang, "Energy-efficient UAV communication with trajectory optimization," *IEEE Trans. Wireless Commun.*, vol. 16, no. 6, pp. 3747–3760, Jun. 2017.

[13] A. R. S. Bramwell, G. Done, and D. Balmford, *Bramwell's Helicopter Dynamics*, 2nd ed. Washington, DC, USA: Amer. Inst. Aeronaut. Astronaut., 2001.